CHRARACTERIZATION OF INTERFACIAL STRENGTH BETWEEN FIBER AND MATRIX BASED ON IMAGE ANALYSIS OF PHOTOELASTICITY

Kosuke Takahashi[1], Bentang A. Budiman[2], Kazuaki Inaba[3] and Kikuo Kishimoto[4]

[1]Division of Mechaical and Aerospace Engineering, Hokkaido University
N13, W8, Kita-ku, Sapporo, Hokkaido, 060-8628, Japan
Email: ktakahashi@eng.hokudai.ac.jp
[2]Mechanical Engineering Department, Institut Teknologi Bandung
Ganesha street no. 10, Bandung 40132, Indonesia
Email: bentang@ftmd.itb.ac.id
[3]Department. of Transdisciplinary Science and Engineering, Tokyo Institute of Technology
2-12-1, Ookayama, Meguro-ku, Tokyo 152-8552, Japan
Email: inaba@mech.titech.ac.jp
[4]Department. of Transdisciplinary Science and Engineering, Tokyo Institute of Technology
2-12-1, Ookayama, Meguro-ku, Tokyo 152-8552, Japan
Email: kkishimo@mep.titech.ac.jp

Keywords: Interfacial strength, Fragmentation, Stress concentrations, Stress transfer, Photoelasticity

Abstract

This study presents a measurement technique of interfacial strength between fiber and matrix based on non-rigid bonding modeled as a cohesive surface. By focusing on the stress concentration near a fiber crack obtained from a single-fiber fragmentation test, the stress contour in matrix visualized by photoelasitic experiment was utilized to characterize the interfacial strength. The primary advantage of this measurement technique is that only a single fiber crack is required, whereas the conventional analysis is based on saturated fiber fragmentation, which is usually obtained in the range of plastic deformation. The stress contours near cracks of as-received and acetone-soaked fibers were observed by photoelasticity. Utilizing polychromatic light, the color values defined in hue, saturated, and value (HSV) system were automatically extracted from each pixel of observed omage by developing simple application software. The results successfully visualized contours of the principal stress difference along the interface, which was generated by a shear traction between fiber and matrix due to fiber crack. Based on the observed stress contour in matrix, maximum value of the traction i.e. interfacial strength was clearly quantified and the decrease in interfacial strength due to acetone treatment was reasonably detected.

1. Introduction

It has been known that composite failure is mainly initiated by interfacial cracks between fiber and matrix, but the characterization of the interface is still a challenging problem. In fact, many failure predictions of the composite presuppose that the interface has a perfect bonding, which means there is no debonding process. For example, single fiber fragmentation test (SFFT), which uses single fiber embedded in a matrix, estimates interfacial strength between fiber and matrix from saturated length of fiber fragmentation. The interface between fiber and matrix is traditionally assumed to be rigid and perfectly transfers load from matrix to fiber. Although it seems simple and straightforward, the

Excerpt from ISBN 978-3-00-053387-7

fragmented fiber length to indicate the interfacial strength might be inappropriate especially by applying simple shearing stress along the interface with perfect bonding assumption.
The weakness of conventional SFFT analysis has been elaborated in line with improvement by many researchers[1, 2]. The proposed improvements are usually based on the fact that a crack from fiber might deflect to the interface rather than penetrate to a matrix. The influence of the interfacial crack has been analyzed using a continuum damage model (CDM), which defines the interface as a non-rigid bonding [3–5]. The interfacial crack is visualized to have a debonding process that traction is gradually decreased until complete separation. The traction distribution along the interface is modeled with traction-separation (t -δ) curve with three parameters called t_0, G_c, and K_0 as shown in Fig. 1. They are interfacial strength which can be achieved at the interface, energy release rate required to make the complete separation of interface, and interfacial stiffness representing non-rigid bonding, respectively.
The problem in CDM-based approach is that there is no comprehensive study to experimentally characterize these properties from SFFT. A direct measurement by characterizing the interface based on CDM is urgently conducted in order to improve the accuracy of estimated interfacial strength. Therefore, an objective of this study is to develop a experimental process of interface characterization considering a debonding process at fiber-matrix interface based on CDM. Our group are proposing a method for evaluating these parameters based on SFFT without requiring the t –δ curve observation [6]. It utilizes a contour of principal stress difference ($\Delta\sigma$) in a matrix, which can be obtained directly via photoelastic analysis. Here, the experiemtal procedure and technique are introduced.

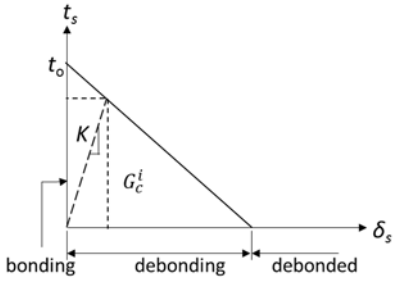

Figure 1. Traction-separation (t -δ) curve on interface.

2. Experiments

2.1. Experimental setup

Specimens used in this study have a square cross section, made of an epoxy resin (KONISHI chemical co. Ltd) and a carbon fiber (HTA40, TOHO Tenax co, LTd). The dimension of the the specimen is shown in Fig. 2a. Two types of specimen were prepared with the different surface treatment of a fiber. The first specimen used as-received fiber with sizing treatment on the surface whereas the other used a conditioned fiber which was soaked in acetone for 5 hours and washed by water to remove adhesive content. Each single fiber was carefully placed into a mold with a load of 0.56 mN applied to the tip of fiber to eliminate fiber miss-alignment during the curing process of epoxy. After they were fully cured, the specimen surfaces were gradually polished by P600, P2000, SC800/2400, and SC1200/4000 sandpapers for 5 minutes each.
An experimental apparatus for photoelastic analysis commonly consists of a light source, a polarizer, two 1/4λ retarders, an analyzer, and a microscope. A high-resolution camera was mounted on the microscopse for recording images.The schematic arrangement of apparatus is shown in Fig. 2b. The specimen placed between two retarders was penetrated by circularly polarized light, which is used to eliminate isoclinic contours. A polychromatic light source is used rather than the monochromatic light source in order to clearly differentiate the principal stress difference ($\Delta\sigma$) contours. The central wave length of 551 nm was used as referenced light of polychromatic wave. When tension is applied to the

Excerpt from ISBN 978-3-00-053387-7

specimen and causes fiber crack, the camera captures an image of isochromatic contours (bright-dark) from the epoxy.

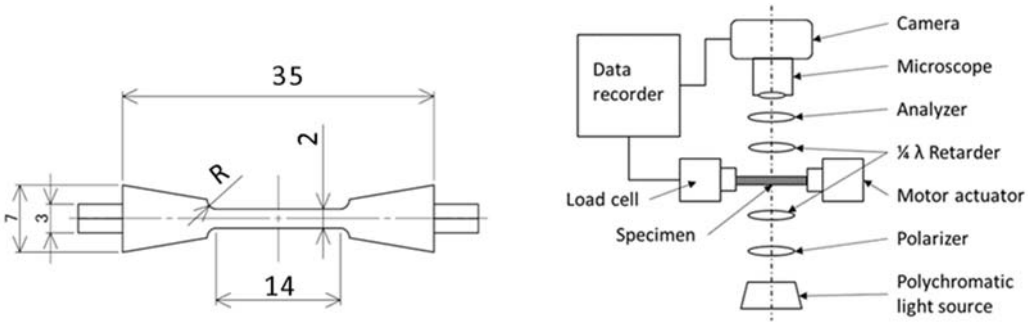

(a) (b)

Figure 2. Specimen size (a) and experimental setup (b).

2.2. Image processing

The contours are generated by optical properties of epoxy as a birefringent material which can have two refractive indexes if the stress appears along the interface due to fiber crack. Those indexes have a relationship with $\Delta\sigma$ following equation below,

$$\Delta\sigma = (f_\sigma N) / h \tag{1}$$

Where f_σ is a stress-optic coefficient, h is specimen thickness, and N is a fringe order related to a retardation of two monochromatic light waves produced by the two refractive indexes.

An image processing technique is introduced by analyzing an image of gradient color obtained in photoelasticity. Our group proposed to apply HSV system for analyzing a photoelastic image. Each image captured by a camera is digitized as a combination of pixels. Each pixel has a unique color defined to be red, green, blue (RGB) or Hue, Saturated, and Value (HSV) systems. Many image processing techniques applied in photoelastic analysis use RGB system to evaluate the color. However, if this system is applied in microscale analysis, it might give a huge error because of the a non-uniform brightness. On the other hand, HSV system separates brightness from color value (hue), which can be solely applied for the photoelastic analysis.

At first, RGB values were extracted from an image of bending tests to evaluate their retardation. A software extracting the color in each pixel by RGB system was developed and applied to images taken by a microscope with high-resolution camera. These RGB values along y axis were expressed as function of N as follow,

$$i(N)=A_i \cos(2\pi/T) + i_{ave} \tag{2}$$

where i is R, G, or B value, A_i is amplitude value, i_{ave} is an average value, and T is a period. Hue value (H) was then calculated by equation (3),

$$H = \begin{cases} 60°\left(\dfrac{\mathrm{G}-\mathrm{B}}{\Delta}\right), & \text{if } i_{max} = \mathrm{R} \\ 60°\left(2+\dfrac{\mathrm{B}-\mathrm{R}}{\Delta}\right), & \text{if } i_{max} = \mathrm{G} \\ 60°\left(4+\dfrac{\mathrm{R}-\mathrm{G}}{\Delta}\right), & \text{if } i_{max} = \mathrm{B} \end{cases} \tag{3}$$

where i_{max} is maximum value among R, G, or B in each pixel.

Excerpt from ISBN 978-3-00-053387-7

2.3. Calibration in photoelasticity

For linear elastic material, the relationship between color gradation and $\Delta\sigma$ can be stated by f_σ. For calibration in photoelasticity, both bending test and tensile test were conducted to assure that f_σ is measured properly. A main advantage of the bending test is that it only requires one image to be analyzed for measuring f_σ. The continuous color can also be captured. However, large deflection might appear particularly near a specimen edge which cause difficulty in determining the stress distribution. On the other hand, stress is distributed uniformly along cross section in tensile test, which usually suitable for material with low elastic modulus. However, obtaining uniform color becomes difficult for high stress condition the calibration. In addition, it requires several images corresponding to its stress.

The schematic details of bending test and tensile test are shown in Figs. 3ab. In bending test, a pure epoxy was placed on a miss alignment with a force line to generate a bending moment as well as a tensile force. As a result, the tension and compression stresses were distributed along cross section (y axis) of the epoxy. Stress distribution along y axis can be obtained by deriving force and moment equilibriums as follow,

$$\sigma_b = (12Fy_0\, y)/h^4 + \sigma_a \tag{4}$$

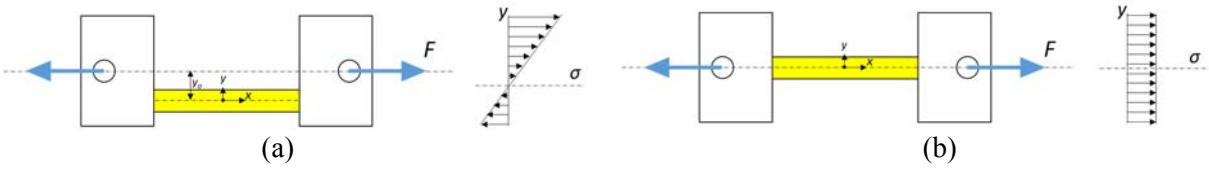

Figure 3. Bending test (a) and tensile test (b) for calibration in photoelasticity.

3. Resuls

3.1. Calibration in photoelasticity

Fig. 4a shows clear sequenced color contours obtained by the bending test when tensile force of 6.2 N was applied. The color contours following Michel-Levy color chart represent stress distribution along y axis. Black color indicates zero stress. Compressed stress occurs below the black color whereas tensile stress occurs on the top of the black color. A sum of bending and tensile stresses is obtained from Eq. (4) as shown in Fig. 4b. This stress is related to the color contours which correspond to N. The color in center region marked by white square line was extracted to obtain RGB values. The RGB values are then plotted in Fig. 5 forming sinusoidal curves. It can be clearly seen that each curve has different frequency so that the RGB combination generates different color depend on its intensity. Table 1 shows parameters obtained from the curves. These values were used for calculating $i(N)$ in Eq. (2), and then Hue function was calculated by Eq. (3). Those functions (H) were also plotted in Fig. 5.

In tensile test calibration, several image with different stress condition were captured as shown in Fig. 6a. The certain specimen area marked by white square line was extracted to RGB system and converted to a Hue value. The averaged Hue value for each σ_a were then obtained. Four epoxy specimens were used for the tensile test calibration, and it was then compared with bending test in Fig. 4b. From Fig. 6b, f_σ of 7.9 MPa.mm was obtained. It can be concluded that both bending and tensile tests generate consistent stress-fringe order curve. Moreover, consistent results also indicate the manufacturing process of epoxy in this study is controlled properly.

Excerpt from ISBN 978-3-00-053387-7

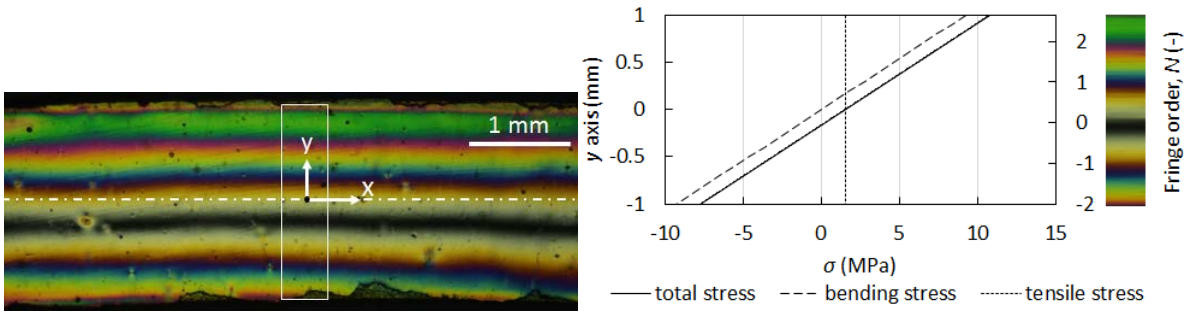

Figure 4. Image of stress contour in bending test (a) and corresponding stress values.

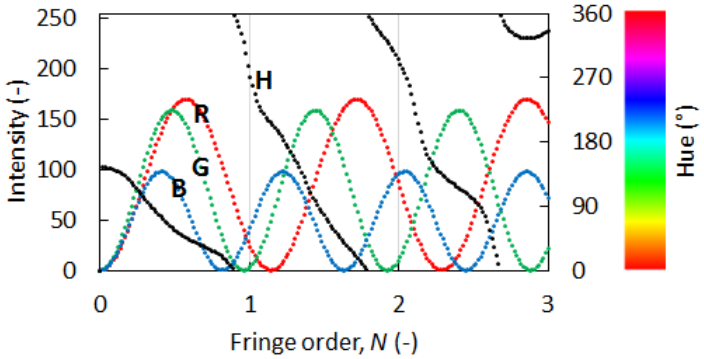

Figure 5. RGB and Hue values corresponding to fringe order.

Table 1. Parameters obtained from RGB values of stress contour to convert to Hue value.

Color	A_i	$i_{avg.}$	T
Red, R	85	85	1.155
Green, G	80	80	0.975
Blue, B	49	49	0.825

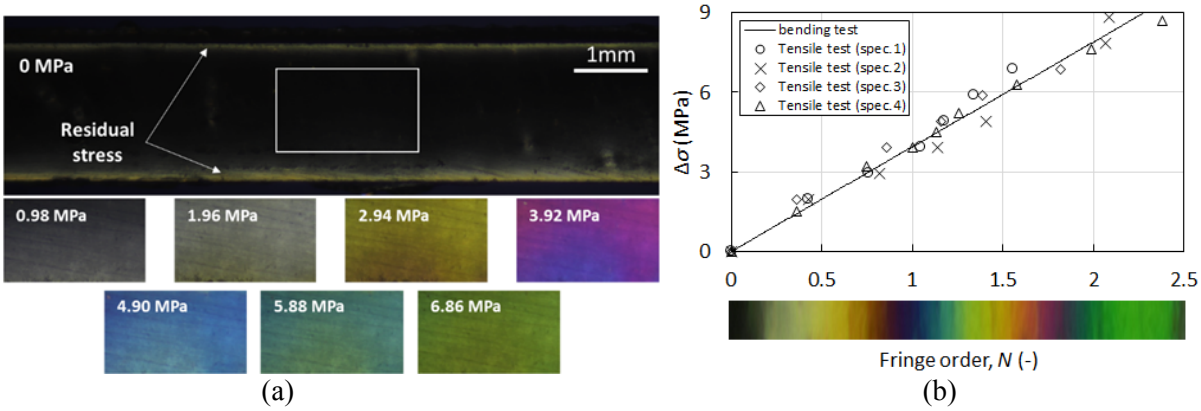

Figure 6. Color change due to uniform tension (a) and comparison with bending test (b).

Excerpt from ISBN 978-3-00-053387-7

3.2. Stress contours near fiber crack

SFFT was conducted to obtain fiber cracks. Figs. 7a and 7b show example images of cracks for as-received fiber and acceton-soaked fiber under certain σ_a. It is seen that shearing stress near the interface creates a color gradation. The acceton-soaked fiber was broken earlier with lower stress (5.9 MPa) than as-received fiber (9.3 MPa). Longer interfacial debonding also appears for the acceton-soaked fiber. The fringe contours for each images were extracted using the developed software and plotted to *r-z* axis as shown in Figs. 8a and 8b. It clearly shows that stress concentration appears near the interface. L_t and L_G for each extracted N were then measured from each black dot. By applying Eq.(1), observed $\Delta\sigma$ at the black dots were also obtained.

In SFFT, projection of light captured by camera is disturbed by axisymmetric effect through the specimen thickness because of the fiber shape. To accommodate this effect, the stress obtained from the photoelastic analysis should be corrected as follows (Schuster & Scala, 1964).

$$\sigma_c = \frac{h(\Delta\sigma - \sigma_a)(b-a)}{2\left\{bm - \frac{1}{2}\left(mb + (a+L_t)^2 log\frac{(m+b)}{(a+L_t)}\right)\right\}} + \sigma_a \qquad (5)$$

$$m = [b^2 - (L_t + a)^2]^{0.5}$$

Eq. (5) was then applied to compensate axisymmetric effect to obtain corrected principal stress difference. Finally, t_0 was obtained from the relationship between $\Delta\sigma$ and the farthest position on each stress contour, indicated by black points in Fig. 10ab. The observation of stress contours was repeated using the other fiber cracks to evaluate the variation of proposed method. As a result. averaged t_0 of 25.8 MPa was calculated for as-received fiber, whereas averaged t_0 of 9.1 MPa was calculated for acceton-soaked fiber. This results conclude that degradation of the interface can also be detected by analysis using proposed method.

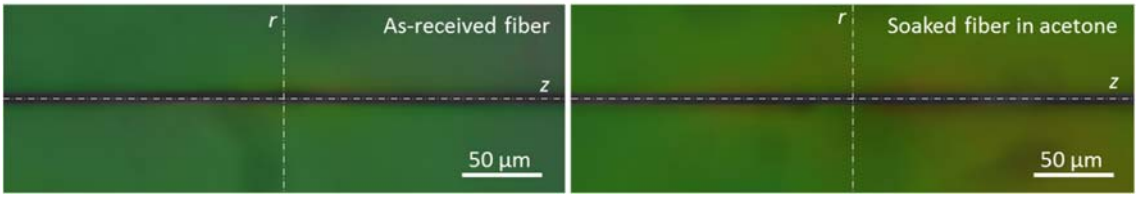

(a) (b)

Figure 7. Photoelastic image of fiber cracks for as-received fiber (a) and acceton-soaked fiber (b).

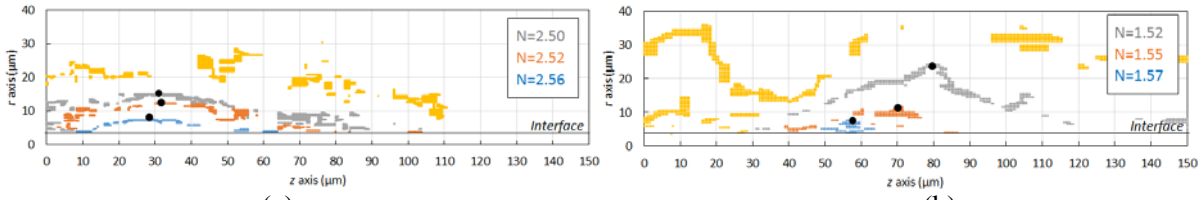

(a) (b)

Figure 8. Extracted stress contours for as-received fiber (a) and acceton-soaked fiber (b)

4. Conclusions

To evaluate the interfacial strength from images of photoelasticity, a method for observing stress field in matrix near an interface was demonstrated. It was realized by developing image processing technique. An intensive discussion for stress-optic calibration was conducted by using bending test and tensile tests. The evaluation of the interfacial strength was conducted using as-received fiber/epoxy specimen and

Excerpt from ISBN 978-3-00-053387-7

conditioned fiber/epoxy specimen, and compared with conventional analysis of SFFT. The results conclude that SFFT successfully differentiates the quality of the interface. Furthermore, overestimating results of the conventional analysis due to the simplicity of the interface model was confirmed.

Acknowledgments

Financial support for this study was provided by a grant from the Mizuho Foundation for the Promotion of Sciences.

References

[1] P. J. Herrera-Franco and L. T. Drzal, Comparison of methods for the measurement of fibre/matrix adhesion in composites, *Composites*, vol. 23, no. 1, pp. 2–27, 1992.

[2] W. A. Curtin, "Exact theory of fibre fragmentation in a single-filament composite," *J. Mater. Sci.*, vol. 26, no. 19, pp. 5239–5253, 1991.

[3] F. Ma and K. Kishimoto, A Continuum Interface Debonding Model and Application to Matrix Cracking of Composites, *JSME Int. journal. Ser. A, Mech. Mater. Eng.*, vol. 39, no. 4, pp. 496–507, Oct. 1996.

[4] C. Shet and N. Chandra, Analysis of Energy Balance When Using Cohesive Zone Models to Simulate Fracture Processes, *J. Eng. Mater. Technol.*, vol. 124, no. 4, pp. 440–450, Oct. 2002.

[5] M. Nishikawa, T. Okabe, and N. Takeda, Determination of interface properties from experiments on the fragmentation process in single-fiber composites, *Mater. Sci. Eng. A*, vol. 480, no. 1–2, pp. 549–557, May 2008.

[6] B. A. Budiman, K. Takahashi, K. Inaba, and K. Kishimoto, A new method of evaluating interfacial properties of a fiber/matrix composite, *J. Compos. Mater.*, vol. 49, no. 4, pp. 465–475, Feb. 2015.

Excerpt from ISBN 978-3-00-053387-7